ePublishing

ΕΘΝΙΚΟ ΚΕΝΤΡΟ ΤΕΚΜΗΡΙΩΣΗΣ
EKT
NATIONAL DOCUMENTATION CENTRE

Journal of the Hellenic Veterinary Medical Society

Vol 73, No 3 (2022)

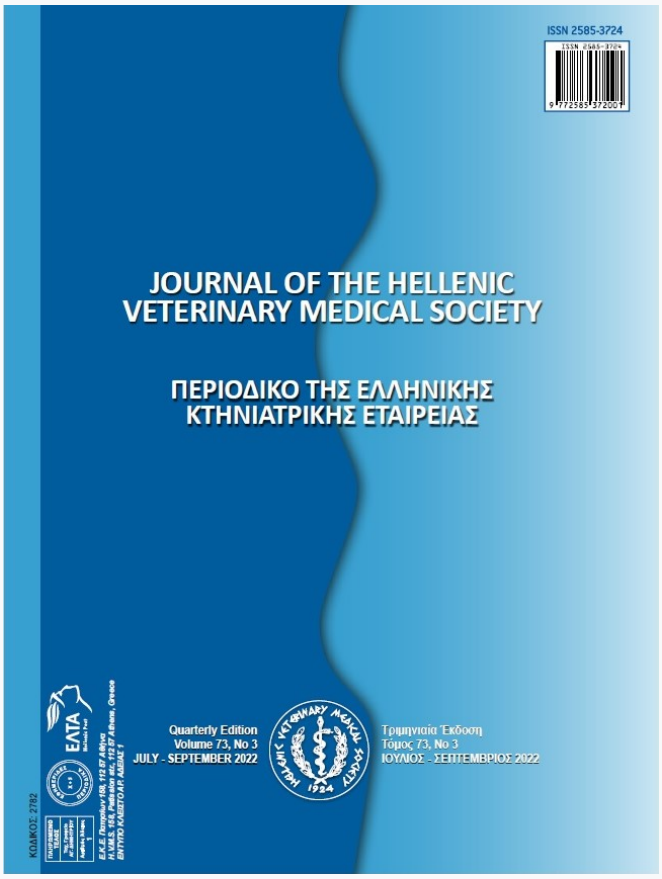

Biometric radiographic features between foot lesions and long toe under-run heel in donkeys

AI El-Marakby, AI Abdelgalil, MB Mostafa, AS Soliman

doi: 10.12681/jhvms.27827

Copyright © 2022, Ahmed Ismael Abdelgalil

This work is licensed under a Creative Commons Attribution-NonCommercial 4.0.

To cite this article:

El-Marakby, A., Abdelgalil, A., Mostafa, M., & Soliman, A. (2022). Biometric radiographic features between foot lesions and long toe under-run heel in donkeys. *Journal of the Hellenic Veterinary Medical Society*, *73*(3), 4559–4566. https://doi.org/10.12681/jhvms.27827

https://epublishing.ekt.gr | **e-Publisher:** EKT | **Downloaded at:** 25/04/2024 08:46:18

J HELLENIC VET MED SOC 2022, 73 (3): 4559-4566
ΠΕΚΕ 2022, 73 (3): 4559-4566

Research article
Ερευνητικό άρθρο

Biometric radiographic features between foot lesions and long toe under-run heel in donkeys

A.I. El-Marakby[1], A.I. Abdelgalil[2,*], M.B. Mostafa[2], A.S.Soliman[2]

[1]Postgraduate master student

[2] Department of Surgery, Anesthesiology and Radiology, Faculty of veterinary medicine, Cairo University. Egypt

ABSTRACT: The present study aimed to document the relationship between biometric foot measurements and different radiographic lesions in 30 donkeys' feet with long toe, under-run heel. The common radiographic foot lesions were pedal osteitis complex in 26 (86.6%) and navicular bone reaction in 8 (26.7%). Osteophyte reaction was identified at the proximal phalanx in 8 (26.7%) and the middle phalanx in 10 (33.3%). Pastern and coffin joints osteoarthritis were found in 4 (13.3%) and 9 (30%) respectively. Palmar soft tissue calcification and fracture of the eminence of 2nd phalanx were reported in 5 (16.6%) and 1 (3.3%) respectively. Positive correlation was recorded between dorsal hoof wall angle (DHWA) and the axis of the distal phalanx, 3rd phalanx, proximal palmar cortex angles, the heel angle, and 3rd phalanx solar border angle. Strong positive correlation was recorded between dorsal hoof wall length (DHWL) and dorsal coronary band height, medial wall length, lateral wall length, lateral coronary band distance, medial coronary band distance, lateral distal phalanx to bottom distance, and medial distal phalanx to bottom distance. The dorsal hoof wall and heel angles reflected increased stress on the hoof capsule, distal interphalangeal joint, navicular bone, and palmar soft tissue structures. The low heel, the decreased distal phalanx solar border angle and under development of the palmar section of the hoof lead to slippage of the third phalanx dorsally, increased tension on the deep digital flexor tendon, navicular bone, and pedal osteitis complex in long toe, under-run heels. This study demonstrated a relationship between biometric foot measurements and the presence of radiographic foot lesions detected in long toe, under-run heel in donkeys.

Keywords: hoof; long toe; under-run heel; radiographic; biometric.

Corresponding Author:
Ahmed Ismael Abdelgalil, Department of Surgery, Anesthesiology and Radiology, Faculty of veterinary medicine, Cairo University. P.O. Box: 12211 Giza
E-mail address: ismael7591@yahoo.com

Date of initial submission: 17-08-2021
Date of acceptance: 05-12-2021

INTRODUCTION

The conformation of the equine hoof is considered an important factor affecting the performance of the horse (Linford et al., 1993). The hoof is a complex modification of the integument surrounding, supporting, and protecting structures within the distal limb of the horse (Dyson et al., 2011a). Long toe, under-run heel in donkeys is a hoof conformation characterized by an increase in toe and heel length, and the dorsal hoof wall appears concave or convex. The hoof capsule appears oblong, the heels move forward, the apex of the frog extends, and the hoof pastern axis appears broken back (Mostafa et al., 2018). The heel horn tubules have been bent and their angle relative to the ground is decreased in long toe, under-run heel (O'Grady, 2020). Additionally, the distorted hoof capsule alters forces applied to the hoof, changes the internal structures of the foot and alters biomechanical function that considered predisposing factors to foot lameness (Holroyd et al., 2013). Radiographic studies of the foot have been used to measure the conformation, shape, angles of the digit (White et al., 2008), and evaluation of hoof injury, and balance (Denoix, 1999). Long toe, under-run heel conformation in front feet has been associated with increase in the extension of the deep digital flexor tendon and distal interphalangeal joint, navicular injuries and suspensory apparatus break down (Kane et al., 1998; Denoix, 1999; Eliashar et al., 2004; Holroyd et al., 2013).

Long toe, under-run heel has been linked to lameness and poor hoof conformation in the horse (O'Grady, 2020). The relationships between the radiographic measurements of foot conformations of equine lameness, in particular, navicular, tendon, and ligament injuries have been studied (Holroyd et al., 2013; De Zani et al., 2016). Limited studies have been published describing the biometric radiographic conformation parameters and foot lesions in long toe, under-run heel in donkeys. Therefore, the objective of the present study was to determine the relationships between biometric foot measurements and different radiographic lesions in a group of donkeys' feet with long toe, under-run heel.

MATERIALS AND METHODS

This study was approved by the institutional animal care and use committee at Cairo University (CU-II/F/32/20). The study was carried out on 30 front hooves obtained from 15 male donkey cadavers affected with long toe, under-run heels. The mean ages were 9.62 ± 3.69 years and the mean body weight was 280.2 ± 11.2 kg. Evaluation of the hoof capsule was carried out from the dorsal, lateral, and palmar aspects, as well as from the solar surface (Mostafa et al., 2018). Standardized radiographs were taken for Lateromedial (LM) and dorsopalmar (DP) projections (Dyson et al., 2011b). The horizontal X-ray beam was centered 2 cm below the coronary band, at the midpoint between the bulbs of the heel and the proximodorsal aspect of the hoof wall, and for DP x-ray beam was centered on the median of the dorsal hoof wall. Radiography was performed using mobile X-ray machine (Fischer). The radiographic setting factors ranged from 50-55 kV, 10 mAs and 90 cm focal spot film distance (FFD).

Lateral and palmar photographic images of the foot were taken using digital camera (KODAK, 8.2 megapixels. China) (White et al., 2008). The digital camera was placed at a standardized distance 50cm from the limbs. The dorsal and palmar aspects of the hoof wall were marked by 2 metal wires. Additionally, a small metal ball was placed just dorsal to the apex of the frog. Both photographic and radiographic images were analyzed using computerized software program (AutoCAD 2019 program). Radiographs for the changes in the foot structures were evaluated (Butler et al., 2017). The radiographic measurements were obtained from lateromedial (LM) (Figure 1) and dorsopalmar (DP) (Figure 2).

Angles

The dorsal hoof wall angle (DHWA), heel angle (HA), 3rd phalanx angle (P3A), 3rd phalanx solar border angle (P3BA), the axis of the distal phalanx angle (LP3A), proximal palmar cortex angle (PPCA) were measured from lateromedial view. The lateral wall angle (LWA) and medial wall angle (MWA) were measured from dorsopalmar view.

Distances

The dorsal hoof wall length (DHWL), dorsal coronary band height (DCBH), and palmar coronary band height (PCBH) were measured from lateromedial view. Medial wall length (MWL), lateral wall length (LWL), lateral coronet to bottom distance (LCBD), medial coronet to bottom distance (MCBD), lateral distal phalanx to bottom distance (P3BL), Medial distal phalanx to bottom distance (P3BM), Distal phalanx to lateral hoof wall distance (P3HL), Distal phalanx to medial hoof wall distance (P3HM) were measured from the dorsopalmar views.

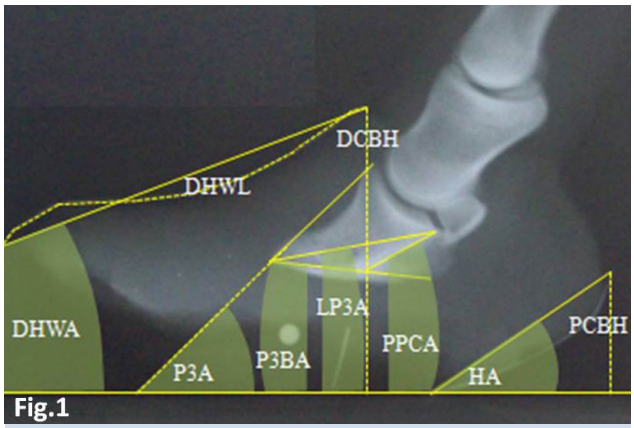

Fig 1: Latero-medial (LM) radiographic measurements of long toe, under-run heel in donkeys: DHWA(Dorsal hoof wall angle), HA(Heel angle), P3A(Distal phalanx angle), P3BA(Distal phalanx solar border angle), LP3A(Axis of distal Phalanx angle), PPCA(Proximal palmar cortex angle); DHWL(Dorsal hoof wall length); DCBH(Dorsal coronary band height); PCBH (Palmar coronary band height).

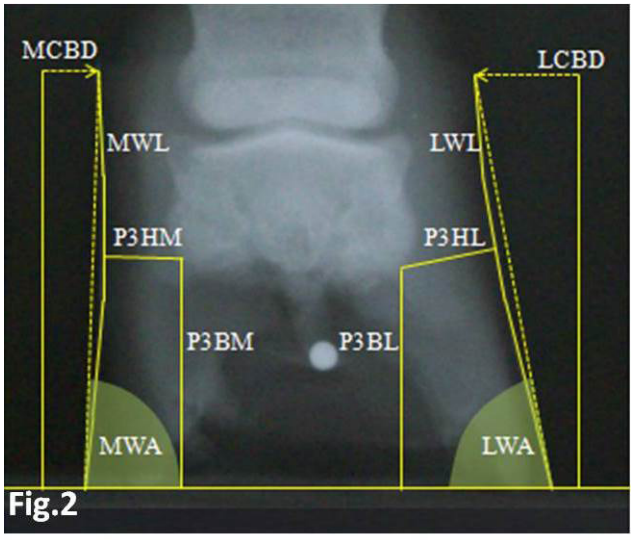

Fig 2: Dorsopalmar (DP) radiographic measurements of long toe, under-run heel in donkeys: MWA(Medial wall angle):; LWA(Lateral wall angle); MWL(Medial wall length); LWL (Lateral wall length); MCBD(Medial coronet to bottom distance); LCBD(Lateral coronet to bottom distance); P3BM(Medial distal phalanx to bottom distance); P3BL(Lateral distal phalanx to bottom distance); P3HM(Distal phalanx to medial hoof wall distance); P3HL(Distal phalanx to lateral hoof wall distance)

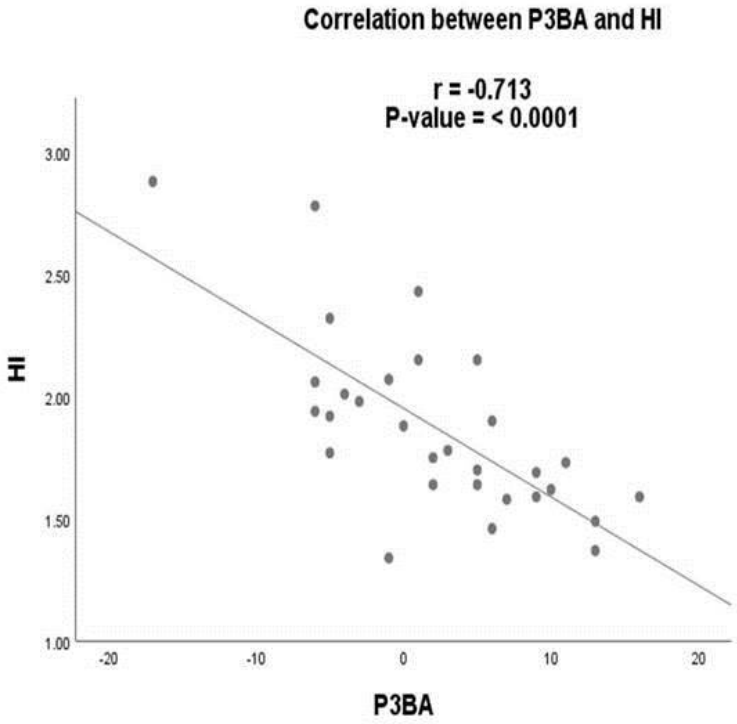

Fig 3: Correlation between P3BA and HI; There is a significant strong negative correlation between P3BA and HI

Ratio

The heel height index (HI) was calculated (Figure 3) as the ratio between dorsal coronary band height (DCBH) and palmar coronary band height (PCBH) (Eliashar et al., 2004). The relationships between the 3rd phalanx solar border angle (P3BA) and Heel height (HI) were calculated to determine the effects of long toe, under-run heel conformation on foot structure lesions in donkeys (Table 1).

Statistical analysis

Data were assessed with a one-sample Kolmogorov–Smirnov test to confirm that there were within normal distribution. Descriptive statistics (mean ± SE, minimum, and maximum) were calculated for all biometric measurements. Correlation between the dorsal hoof wall angle, the dorsal hoof wall length, and all other biometric measurements were analyzed by Pearson Correlations using SPSS 19 (IBM). Significance was set at $P < 0.05$.

RESULTS

In the current study, the radiographic findings associated with long toe under run heel conformation were pedal osteitis complex in 26 feet (86.6%), the navicular bone reaction in 8 feet (26.7%), osteophyte reaction at 1st phalanx in 8 feet (26.7%) and 2nd phalanx in 10 feet (33.3%), pastern OA in 4 feet (13.3%), coffin OA in 9 feet (30%), palmar soft tissue calcification in 5 feet (16.6%), and fracture of 2nd phalanx in 1 foot (3.3%).

The distal phalanx pedal osteitis complex included osteophyte reaction (Figure 4 a & c) at the articular border of P2 and P3 (Coffin joint osteoarthritis). Enthesophyte reactions at the dorsal and palmar process of P3, severe osteolytic changes at the solar margin of P3 (Figure 4 b), and ill-defined osseous cyst-like lesions within the solar margin of P3 were determined (Figure 4d).

The navicular bone showed enthesophyte formation at the proximal and palmar borders with marked

Table 1. Mean ± SE, minimum, maximum, and correlations to assess the relationship between the dorsal hoof wall angle, dorsal hoof wall length and the biometric radiographic lesions in long toe, under-run heel in donkeys

Measurement parameters	Mean ± SE	Min	Max	Correlation coefficient			
				DHWA		DHWL	
				(r_s)	*P*-value	*r*	*P*-value
Dorsal hoof wall angle "DHWA"	48.73 ˚ ± 1.567 ˚	20 ˚	57 ˚	1.000	——	**-0.564****	**0.001**
Heel angle "HA"	45.03 ˚ ± 1.399 ˚	31 ˚	62 ˚	0.557**	0.001	**-0.546****	**0.002**
3rd phalanx angle "P3A"	52.7 ˚ ± 1.126 ˚	39 ˚	64 ˚	0.657**	≤0.0001	**-0.627****	**≤0.0001**
3rd phalanx solar border angle "P3BA"	2.17 ˚ ± 1.335 ˚	-17 ˚	16 ˚	0.596**	0.001	**-0.51****	**0.004**
Axis of distal phalanx angle "LP3A"	21.2 ˚ ± 1.178 ˚	6 ˚	32 ˚	0.729**	≤0.0001	**-0.583****	**0.001**
Proximal palmar cortex angle "PPCA"	35.63 ˚ ± 1.302 ˚	21 ˚	46 ˚	0.815**	≤0.0001	**-0.488****	**0.006**
Dorsal hoof wall length "DHWL" (mm)	69.71 ± 1.689	52.9	95.13	-0.564**	0.001	——	——
Dorsal coronary band height "DCBH" (mm)	57.95 ± 1.194	46.6	73.04	-0.318	0.086	**+0.889****	**≤0.0001**
Palmar coronary band height "PCBH" (mm)	31.87 ± 1.154	19.21	47.72	0.197	0.297	**+0.231**	**0.219**
Heel height index "HI" (DCBH: PCBH)	1.87 ± 0.068	1.34	2.88	-0.357	0.053	**+0.318**	**0.087**
Medial wall angle "MWA"	86.63 ˚ ± 1.098 ˚	65 ˚	95 ˚	-0.172	0.364	**-0.137**	**0.47**
Lateral wall angle "LWA"	87.97 ˚ ± 0.981 ˚	78 ˚	102 ˚	0.130	0.495	**-0.046**	**0.808**
Medial wall length "MWL" (mm)	53.67 ± 1.608	39.67	74.64	-0.398*	0.029	**+0.752****	**≤0.0001**
Lateral wall length "LWL" (mm)	52.97 ± 1.403	38.24	71.61	-0.402*	0.028	**+0.79****	**≤0.0001**
Lateral coronet to bottom Distance "LCBD" (mm)	52.53 ± 1.363	38.24	71.54	-0.411*	0.024	**+0.796****	**≤0.0001**
Medial coronet to bottom Distance "MCBD" (mm)	53.05 ± 1.471	39.66	71.54	-0.408*	0.025	**+0.788****	**≤0.0001**
Lateral distal phalanx to bottom distance "P3BL" (mm)	26.94 ± 1.244	15.66	43.59	-0.545**	0.002	**+0.84****	**≤0.0001**
Medial distal phalanx to bottom distance "P3BM" (mm)	27.52 ± 1.247	15.66	41.73	-0.577**	0.001	**+0.826****	**≤0.0001**
Distal phalanx to lateral hoof wall distance "P3HL" (mm)	12.06 ± 0.442	5.25	16.58	0.112	0.556	**+0.253**	**0.177**
Distal phalanx to medial hoof wall distance "P3HM" (mm)	11.89 ± 0.396	8.07	15.31	0.166	0.381	**+0.27**	**0.149**

SE: standard error
DHWA:dorsal hoof wall angle
DHWL:dorsal hoof wall length

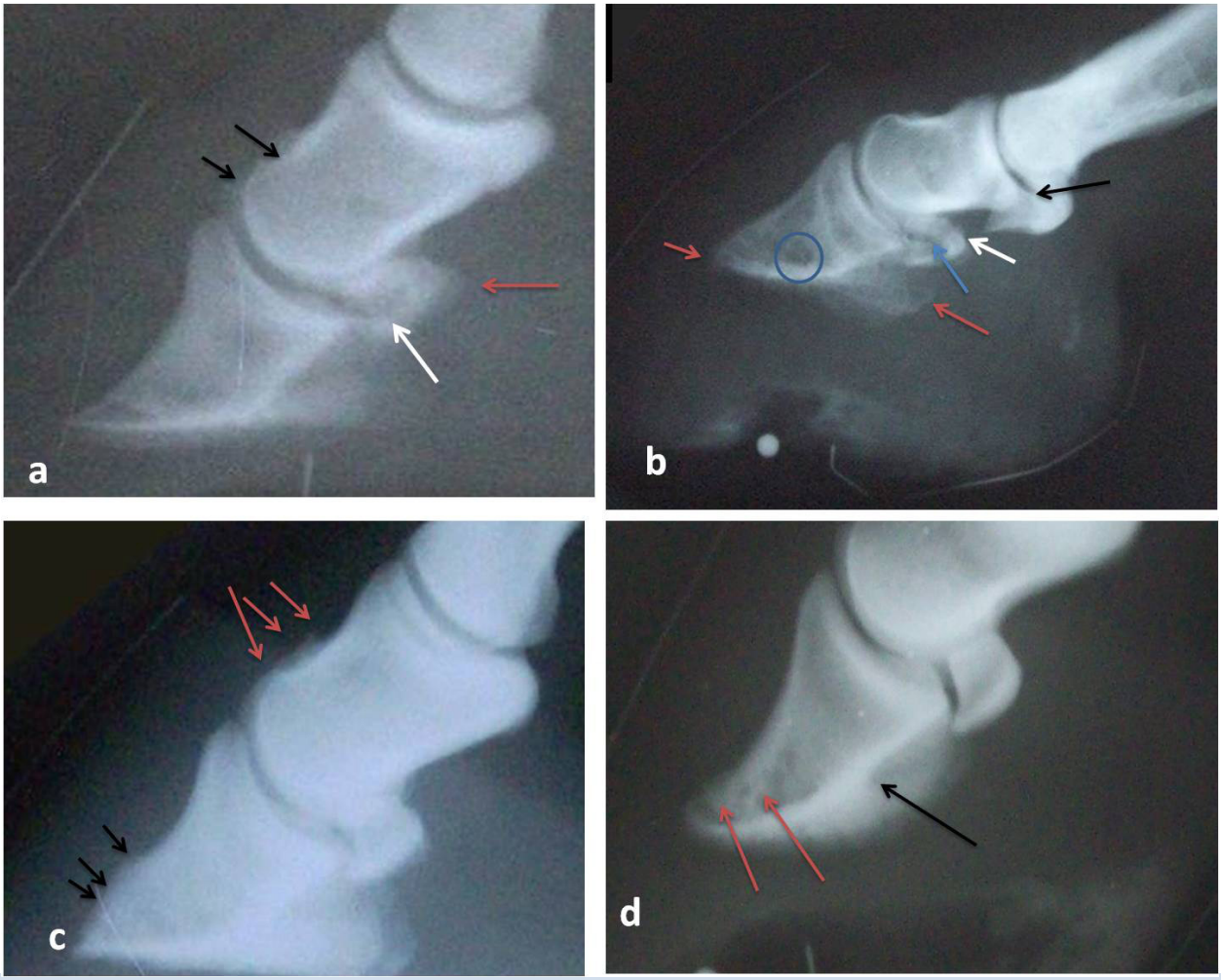

Fig 4: Latero-medial radiographic views of feet with long toe, under-run heels. Fig 4 a: showed enthesiophyte reaction at dorso distal border of the2nd phalanx with coffin osteoarthritis (black arrows). Enthesiophyte reaction at proximal and palmar borders of the navicular bone (red arrows) with remarkable bone resorption (white arrow). Fig 4b: revealed fracture at proximal eminence of the 2nd phalanx (black arrow), enthesiophyte reaction at dorsal and palmar process of 3rd phalanx (red arrows) with osteolytic changes at solar margin (circle) , enthesiophyte reaction at proximal surface of navicular bone (white arrow) with marked radiolucent bone resorption within the navicular bone (blue arrow). Fig 4c: showed new bone formation at the tip of the 3rd phalanx (black arrows) with osteophyte reaction at distal aspect of the 2nd phalanx (coffin O.A) Red arrows. Fig 4d: revealed ill- defined osseous cysts at the tip and solar margin of the 3rd phalanx (red arrows) and osteophyte reaction at palmar process of 3rd phalanx (black arrows)

resorption in the spongiosa of the bone (Figure 4 a, b). Enthesophytes formation at the dorso-distal border of the distal P1 and proximal P2 were seen associated with fracture of the proximal eminence of P2 (Figure 4b& 5). Palmar soft tissue calcifications at the lateral and medial aspect of P2 and osseous cyst at the distal surface of P1 were also detected (Figure 5).

The dorsal hoof wall angle (48.7 ± 1.56˚), heel angle (45.0 ± 1.39˚), 3rd phalanx angle (52.7 ± 1.126˚), 3rd phalanx solar border angle (2.17 ± 1.33˚), the axis of the distal phalanx angle (21.2 ± 1.17˚), the medial wall angle (86.6 ± 1.09˚), and the lateral wall angle (87.9 ± 0.98˚) are presented in table 1.

The mean values for the dorsopalmar measurement parameters were higher for the medial wall angle (MWA), medial coronet to bottom distance (MCBD), medial distal phalanx to bottom distance (P3BM), however, the distal phalanx to lateral hoof wall distance (P3HL) was higher than the medial one (P3HM). The mean value of dorsal coronary band height (DCBH) was greater (57.95 ± 1.194) than the PCBH (31.87 ± 1.154) in lateromedial measurements (Table 1).

The correlation coefficients between the dorsal hoof wall angle (DHWA) and dorsal hoof wall length (DHWL) in long toe, under-run heels are presented in table 1. A strong positive correlation was recorded between DHWA and axis of the 3rd phalanx angle

Fig 5: Dorsopalmar view showed Soft tissue calcifications were noticeable at lateral and medial aspects of the 2nd phalanx which may be mineralization of the collateral sesamoidean ligaments (blue arrows).Osteophyte reaction at the articular border of the distal 2nd phalanx and proximal 3rd phalanx (coffin O.A) Red arrows and radiolucent bone cyst at distal end of the 1st phalanx (circle)

(r=0.729, P ≤0.0001), 3rd phalanx angle (r= 0.657, P ≤0.000), and proximal palmar cortex angle (r= 0.815, P≤0.0001). While the DHWA had a positive, modest correlation with the heel angle (r= 0.557, P≤0.0001), the 3rd phalanx solar border angle (r= 0.596, P = 0.001), and negative correlation with the heel index (HI) (r= -0.357, P= 0.053) (Table 1).

Table 1 showed the correlation coefficients between the increased dorsal hoof wall length (DHWL) and the measured radiographic parameters. The DHWL had a negative, modest correlation with DHWA, HA, P3A (r= - 0.627, p ≤0.0001), P3BA, the axis of the distal phalanx (LP3A), and PPCA. A strong positive correlation was recorded between DHWL and dorsal coronary band height (r= + 0.752, P ≤0.0001), MWL, LWL, LCBD, MCBD, lateral distal phalanx to bottom distance, P3BM. The palmar cortex length had a positive, modest correlation with DHWL.

Weak, negative correlation was found between HI and DHWA (r= -0.357, P= 0.05). Strong negative correlation was found between the HI and the 3rd phalanx solar border angle (*r= -0.713, P ≤ 0.0001*).

DISCUSSION

In the present study, the dorsal hoof wall angle (48.73˚± 1.567˚) and heel angle (45.03 ˚ ± 1.399˚) values were smaller compared to previous studies. Previous guidance for donkey's healthy hooves was 58.25˚, and 54.71 ˚ (Mostafa et al., 2020). It has been reported that the decrease in the DHWA and heel angles increases the stress on the hoof capsule, navicular bone and increases the extension of the distal interphalangeal joint (Hinterhofer et al., 2000; Moleman et al., 2006). Likewise, long DHWL in a Warm-blood horse is associated with smaller DHWA before trimming (Kummer et al., 2006). The same was observed in this study; there was a negative, modest correlation between DHWL and DHWA (*r* = -0.564; *P*-value = 0.001). Furthermore, changes in the shape of the hoof alter the maximal flexion and extension of the distal interphalangeal joint and affect the biomechanics of the whole foot (Chateau et al., 2006). Therefore, the observed bone reactions at the dorsal surface, palmar processes, and the solar margin of P3 were detected radiographically. The remodeling of the dorsal wall of P3 was attributed to pedal osteitis complex associated with long toe, low heel condition due to irregular roughening of the P3 surface (Dyson et al., 2011; Butler et al., 2017).

Previous studies have shown that the distal interphalangeal joint during movement is subjected to different stresses on the articular surfaces and the tendo-ligamentous structures (Denoix, 1999; Clayton et al., 2007). In addition, an unbalanced foot increases the compressive forces on the DDFT, collateral ligaments, distal sesamoidean impair ligaments, and navicular bone (Wilson and Weller, 2011). Increased DHWL, decreased DHWA and low heel angle increase stresses in the palmar foot, shift weight bearing on the palmar section of the foot, and increase strain on the DDFT and navicular apparatus (O'Grady, 2020). Therefore, radiographic foot lesion structures in the present study have collaborated with the previous findings (Denoix, 1999; Eliashar et al., 2004; Wilson and Weller, 2011; O'Grady, 2020).

In the present study, the decrease in the DHWA was associated with decrease in the P3A, LP3A, and PPCA. However, a previous study revealed increase in these parameters in donkeys with laminitis that was attributed to the change in anatomical position of the distal phalanx (Collins et al., 2011). In the present study, the decrease in these parameters was mainly attributed to the dorsal slippage and reverse rotation

of the distal phalanx. Similarly, O'Grady (2013) suggested the dorsal movement of the distal phalanx in long toe, under-run heels in horses. Moreover, a negative value of the 3rd phalanx solar border angle (P3BA) indicates the decrease in the palmar soft tissue structures of the foot (O'Grady, 2020). Besides, the compromised structures of the palmar section of the foot allow the palmar margins of the distal phalanx to descend distally. Consequently, in the present study, the orientation of the distal phalanx was slightly slipping dorsally in long toe, under-run heels and collaborated with O'Grady's results (2013) in the horse.

In the present study, P3BA was positively correlated with DHWA. It has been reported that the palmar solar border is lower in the under-run heel (O'Grady, 2020). Hyperextension of DIP joint, navicular bone shifting proximally toward the palmar surface of P2 and the dorsal slippage of distal phalanx due to the negative palmar angle syndrome were documented (Floyd, 2010). The same findings in the present study coincided with previously reported results (Floyd, 2010; O'Grady, 2020).

The correlation between the small solar angle, low heels and DDFT and navicular bone injuries have been described (Holroyd et al., 2013). Recently the relationship between radiographic measurements of the foot and the presence of lesions detected on MRI has been documented (De Zani et al., 2016). Consequently, in the present study, the relationship between the biometric measurements of the DHWA and the presence of foot lesions documented the alterations of distal phalanx pedal osteitis complex, navicular injuries, dorsal slippage of the distal phalanx and negative palmar angle syndrome, and palmar soft tissue calcification.

In the current study, DHWL had a negative correlation with P3BA, heel angle, P3A, LP3A, and PPCA. The decrease in P3BA increases the force of DDFT on the navicular bone (Eliashar et al., 2004). The P3BA is dependent on the conformation of the palmar section of foot (O'Grady, 2020). The P3BA and DHWA have been decreased with lameness in horse (Dyson et al., 2011b). Similarly, the same findings were observed in the current study on donkeys with long-toe under-run heels.

Toe length influences the moment of force applied on the DIPJ and increases the loading of the navicular bone (Wilson and Weller, 2011). Relationships were found in the current study between long dorsal hoof wall length and injuries of the deep digital flexor tendon, enthesophyte formation at insertion sites of the collateral sesamoidean ligament, distal sesamoidean ligaments, navicular spongiosa and navicular bone proximal border (Dyson et al., 2011; Dyson et al., 2011b).

In the present study, a negative strong correlation was found between the heel index and the 3rd phalanx solar border angle. Thus, this study supports previous research that HI was related to DDFT and navicular bone injuries (Eliashar et al., 2004; Holroyd et al., 2013). Increased DHWL in the present study was positively correlated with MWL, LWL, LCBD, MCBD, P3BL, and P3BM. O'Grady (2013) reported an increase in these parameters is associated with increase in the stresses or weight-bearing placed on a section of the hoof capsule, changes the position of the coronary band and hoof growth rate as well as deviate the hoof wall.

Increased DHWL increases the stress on the palmar foot contributing to palmar foot pain and accelerates the degenerative changes within the coffin joint (Redding, 2007; O'Grady, 2013). Therefore, pastern and coffin osteoarthritis in the present study could be attributed to poor hoof conformation, imbalance of foot, and overstress in long toe, under-run heels.

Osseous cyst-like lesions were observed at the insertion of the collateral ligaments of the distal interphalangeal joint, insertion of the distal sesamoidean impar ligament, and weight-bearing surface of the distal phalanx (Mostafa et al., 2020). Similarly, osseous cyst-like lesions were recorded in the current study. Furthermore, trauma may lead to bone ischemia and necrosis, revascularization, and resorption of necrotic bone leaving a subchondral lesion (Verschooten and Moor, 1982).

CONCLUSIONS

Radiographic and biometric foot lesions associated with long toe, under-run heel were presented. Pedal osteitis complex, navicular bone reaction, osteoarthritis in the pastern, and coffin joints, irregular proximal and palmar surfaces of the navicular bone and navicular spongiosa, osseous cyst-like lesion within the solar margin of P3 and palmar soft tissue calcification were documented.

Correlations were found between various biometric measurements and radiographic foot lesion in long toe, under-run heel in donkeys. The increased dorsal

hoof wall length and the decreased dorsal hoof and heel angles reflected increase in the stress on the hoof capsule, distal interphalangeal joint, navicular bone, and palmar soft tissue structures. The low heel, the decrease in the 3rd phalanx solar border angle and under development of the palmar section of the hoof lead to slippage of the third phalanx dorsally, increase tension on the DDFT and navicular bone, and pedal osteitis complex in long toe, under-run heels.

The increase in DHWL is commonly associated with increase in the stress on the palmar foot section contributing to unbalanced foot and alterations on palmar foot and DIPJ structures. This study proved a relationship between radiographic measurements of the foot and the presence of radiographic lesions in long toe, under-run heel in donkeys.

REFERENCES

Butler J, Colles C, Dyson S, Kold S, Poulos P (2017) Foot, pastern, and fetlock. In: Clinical Radiology of the Horse. 4th ed, Wiley-Blackwell, Oxford, UK: pp 53– 187

Chateau H, Degueurce C, Denoix JM (2006) Three-dimensional kinematics of the distal forelimb in horses trotting on a treadmill and effects of elevation of heel and toe. Equine Vet J 38:164-169.

Clayton H M, Sha D H, Stick J A and Robinson P (2007) 3D kinematics of the interphalangeal joints in the forelimb of walking and trotting horses. Vet Comp Orthop Traumatol 20: 1-7.

Collins SN, Dyson S J, Murray RC, Burden F, Trawford A (2011) Radiological anatomy of the donkey's foot: objective characterization of the normal and laminitic donkey foot. Equine Vet J 43: 478-486.

De Zani D, Polidori C, di Giancamillo M , Zani DD (2016) Correlation of radiographic measurements of the structures of the equine foot with lesions detected on magnetic resonance imaging. Equine Vet J 48:165-171.

Denoix JM (1999) Functional anatomy of the equine interphalangeal joint. Proc. Am. Ass. Equine Pract 45:174-177.

Dyson S, Murray R, Schramme M, Blunden T (2011) Current concepts of navicular disease. Equine Vet. Educ 23 :27-39.

Dyson SJ, Tranquille CA, Collins SN, Parkin TDH and Murray RC (2011a) External characteristics of the lateral aspect of the hoof differ between non-lame and lame horses. Vet J 190: 367-371.

Dyson SJ, Tranquille CA, Collins SN, Parkin TDH, Murray RC (2011b) An investigation of the relationships between angles and shapes of the hoof capsule and the distal phalanx. Equine Vet J 43: 295-301.

Eliashar E, McGuigan MP, Wilson AM (2004) Relationship of foot conformation and force applied to the navicular bone of sound horses at the trot. Equine Vet J 36: 431–435.

Floyd AE (2010) Use of a grading system to facilitate treatment and prognosis in horses with negative palmar angle syndrome (Heel collapse): 107 cases. J equine vet Sci 30(11): 666-675.

Hinterhofer C, Stanek C, Haider H (2000) The effect of flat horseshoes, raised heels and lowered heels on the biomechanics of the equine hoof assessed by finite element analysis (FEA). J Vet Med A 47: 73-82.

Holroyd K, Dixon JJ, Mair T, Bolas N, Bolt DM, David F (2013) Variation in foot conformation in lame horses with different foot lesions. Vet J 195: 361-365

Kane AJ, Stover SM, Gardner IA, Bock KB, Case JT, Johnson BJ, Anderson ML, Barr BC, Daft BM, Kinde H, Larochelle D, Moore J, Mysore J, Stoltz J, Woods L, Read DH, Ardans AA (1998) Hoof size, shape, and balance as possible risk factors for catastrophic musculoskeletal injury of Thoroughbred racehorses. Am J Vet Res 59:1545-1552.

Kummer M, Geyer H, Imboden I, Auer J, Lischer C (2006) The effect of hoof trimming on radiographic measurements of the front feet of normal Warmblood horses. Vet J 172:58-66

Linford RL, O'Brien TR, Trout DR (1993) Qualitative and morphometric radiographic findings in the distal phalanx and digital soft tissues of sound Thoroughbred racehorses. Am J Vet Res 54: 38-51.

Moleman M, van Heel MC, van Weeren PR, Back W (2006) Hoof growth between two shoeing sessions leads to a substantial increase of the moment about the distal, but not the proximal, interphalangeal joint. Equine Vet J 38: 170-174.

Mostafa MB, Abdelgalil AI, Farhat SF (2018) Preliminary assessment of hoof deformities in donkeys. J. Egypt Vet Med Assoc 78 (Apr): 641-654.

Mostafa MB, Abdelgalil AI, Farhat SF, Raw Z, Kubasiewicz LM (2020) Morphometric measurements of the feet of working donkeys Equus asinus in Egypt. J. Equine Sci 31(Feb):17-22.

O'Grady SE (2013) How to evaluate the equine hoof capsule. In: 59th American Association of Equine Practitioners Proceedings, Nashville, TN, USA: 54–61.

O'Grady SE (2020) Foot care and farriery. In: Adams and Stashak's lameness in horses. 7th ed, John Wiley & Sons, Inc: pp 1091-1133.

Redding W (2007) Pathologic conditions involving the internal sturctures of the foot. In: Equine Podiatry, 1st ed, Saunders, St. Louis :pp 253-293.

Verschooten F, De Moor A (1982) Subchondral cystic and related lesions affecting the equine pedal bone and stifle. Equine vet J 14: 47-54.

White JM, Mellor DJ, Duz M, Lischer CJ, Voute LC (2008) Diagnostic accuracy of digital photography and image analysis for the measurement of foot conformation in the horse. Equine Vet J 40: 623-628.

Wilson A, Weller R (2011) The biomechanics of the equine limb and its effect on lameness. In: Diagnosis and Management of Lameness in the Horse, 2nd ed, W.B. Saunders Co., Philadelphia: pp 270-281.